Complete Sensor Fusion System

Raiyan Faruqui and Kevin Qiu
Department of Mechanical and Mechatronics Engineering
University of Waterloo
Waterloo, Canada
rfaruqui@uwaterloo.ca, longlai.qiu@uwaterloo.ca

I. Introduction

While utilizing sensor systems to simply collect data can be beneficial in certain research or troubleshooting scenarios, there are often no real benefits in a commercial application where the relationship between cost and reward is much more strict. However, when these systems are utilized to perform some sort of decision-making such as locating a physical object, their value becomes much more clear. A prime example of this is the autonomous vehicle, where sensors are utilized all around the vehicle to not only form an accurate representation of the world around itself as it drives, but also to perform key decisions that a human operator may not be able to do.

In this lab, sensors are used to locate a heat source produced by a Peltier module on a two-dimensional aluminum plate. Both infrared sensors and thermocouples are implemented in the experiment, both separately and as a combined sensor fusion system. The purpose of this lab is threefold: 1) to implement a complete sensor fusion with multiple levels of sensor complexity, 2) to fuse data from different sensor types, and 3) to perform effective decision making techniques to identify a heat source. Both simulations and experimental implementations of multiple scenarios were evaluated and compared.

First, the thermocouple sensors are characterized to develop a sensor model for voltage with respect to distance. This model joins the previously determined infrared (IR) sensor models to form the complete system model. Simulation and experimental tests are developed to locate the heat source in a 10 cm by 10 cm plate using solely IR sensors, solely thermocouples, and then a combination of the two. In each case, the simulation and experimental localizations were compared.

II. Sensor Model Characterization

A k-type thermocouple along with Adafruit's AD8495 amplifier were used to characterize the thermocouple sensor model. This was achieved by recording voltage measurements at known distances of 1, 3, 5 and 8 cm from the heat source. Voltage measurements were recorded for 5 seconds at a frequency of 8000 Hz using a NI ELVIS II+ board. The aluminum plate was allowed to cool for 10 minutes between each interval to achieve steady state room temperature. The average voltage value was recorded at each distance and plotted in the figure below.

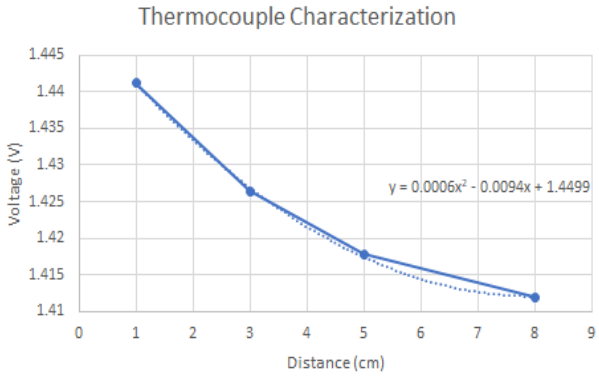

Fig. 1. Thermocouple chracterization plot

Similar to the IR sensors, there exists inherent noise in the system that affects the output signal of the thermocouple. This noise may be attributed to the sensitivity of the sensor and external variables within the lab environment. The final measurement model is shown below which includes additive Gaussian noise to model the sensor noise at zero mean and fixed variance. The variance was obtained from the dataset recorded at 3 cm from the heat source.

$$y_{TC}(d) = 0.0006d^2 - 0.0094d + 1.4499 + N(0, 7.09E-7)$$

III. Simulation

A localization algorithm has to be developed to accurately estimate the location of the heat source on the metal plate. This is assisted with several sensors that have been provided including four IR range sensors and five thermocouples. Three different configurations each with its own extended Kalman filter (EKF) model will be used to localize the heat source. The first configuration uses only IR sensors to estimate the position of the heat source. The second configuration localizes the heat source using thermocouples and the third configuration combines data from both sensors to form a complete sensor fusion system.

Between these three different sensor configurations, the sensor and measurement definitions must be updated in the EKF. The following formulations show only the EKF implementation for the complete system. The simulation code accounts for the different sensor configurations by automatically modifying the EKF according to the desired configuration. The simulation code was developed in MATLAB.

The first step in formulating the EKF is to define the state vector. The state vector has been defined below where X_k represents the position of the centroid of the heat source along the x-axis. Similarly, Y_k represents the position along the y-axis.

$$\begin{bmatrix} x_{1,k} \\ x_{2,k} \end{bmatrix} = \begin{bmatrix} X_k \\ Y_k \end{bmatrix}$$

Kinematics can then be applied to develop a state-space model of the motion of the heat source. Since the position of the heat source will not vary with time, the state vectors at the following time step will be equivalent to that of the current. The covariance matrix Q associated with the state-space model is also defined below. The covariance values were estimated to be relatively low due to the unlikely presence of external factors such as vibration or random motion. The final state-space model is demonstrated as the following:

$$\begin{bmatrix} x_{1,k+1} \\ x_{2,k+1} \end{bmatrix} = \begin{bmatrix} 1 & 0 \\ 0 & 1 \end{bmatrix} \begin{bmatrix} x_{1,k} \\ x_{2,k} \end{bmatrix} + N(0, Q) \qquad Q = \begin{bmatrix} 0.01 & 0 \\ 0 & 0.01 \end{bmatrix}$$

The next step is to define the measurement models for each of the different types of sensors (short [2], medium [3] and long [4] range). From the previous labs, the IR sensor models have been developed as a function of distance (in centimeters) as shown below.

$$y_{short}(d) = 4.55\text{E} - 3d^2 - 0.236d + 3.34 + N(0, 5.75E - 6)$$
$$y_{mid}(d) = 7.4\text{E} - 4d^2 - 0.0932d + 2.96 + N(0, 3.49E - 6)$$
$$y_{long}(d) = 2.18\text{E} - 4d^2 - 0.0527d + 3.23 + N(0, 5.67E - 5)$$

Finally, a 9x1 matrix of the measurement vector can be obtained of the model which features four IR sensors and five thermocouples. It is important to note that the IR sensor models require the state vectors as inputs, whereas the thermocouple models requires distance which is a function of the state vectors as inputs. Additionally, two short range sensors are placed vertically and only require $x_{2,k}$ as input, whereas the mid and long range sensors are placed horizontally, thus requiring $x_{1,k}$ as input. The measurement vector and distance equation are highlighted below.

$$d_i(x_k) = \sqrt{\left(X_k - x_{1,k}\right)^2 + \left(Y_k - x_{2,k}\right)^2}$$

$$h(x_k) = \begin{bmatrix} 7.4\text{E} - 4{x_{1,k}}^2 - 0.0932x_{1,k} + 2.96 \\ 2.18\text{E} - 4{x_{1,k}}^2 - 0.0527x_{1,k} + 3.23 \\ 4.55\text{E} - 3{x_{2,k}}^2 - 0.236x_{2,k} + 3.34 \\ 4.55\text{E} - 3{x_{2,k}}^2 - 0.236x_{2,k} + 3.34 \\ 0.0006\, d_5(x_k)^2 - 0.0094\, d_5(x_k) + 1.4499 \\ 0.0006\, d_6(x_k)^2 - 0.0094\, d_6(x_k) + 1.4499 \\ 0.0006\, d_7(x_k)^2 - 0.0094\, d_7(x_k) + 1.4499 \\ 0.0006\, d_8(x_k)^2 - 0.0094\, d_8(x_k) + 1.4499 \\ 0.0006\, d_9(x_k)^2 - 0.0094\, d_9(x_k) + 1.4499 \end{bmatrix}$$

Due to the nonlinear nature of the sensor models. They must be linearized in order to implement in the EKF. Each measurement is linearized with respect to the state variables by taking the Jacobian. The result is a 9x2 matrix described below.

$$T_i(x_k) = \frac{0.0094}{d_i(x_k)} - 0.0012$$

$$H_k = \begin{bmatrix} 1.48E - 3x_{1,k} - 0.0932 & 0 \\ 4.36E - 4x_{1,k} - 0.0527 & 0 \\ 0 & 9.1E - 3x_{2,k} - 0.236 \\ 0 & 9.1E - 3x_{2,k} - 0.236 \\ T_5(x_k)(X_k - x_{1,k}) & T_5(x_k)(Y_k - x_{2,k}) \\ T_6(x_k)(X_k - x_{1,k}) & T_5(x_k)(Y_k - x_{2,k}) \\ T_7(x_k)(X_k - x_{1,k}) & T_5(x_k)(Y_k - x_{2,k}) \\ T_8(x_k)(X_k - x_{1,k}) & T_5(x_k)(Y_k - x_{2,k}) \\ T_9(x_k)(X_k - x_{1,k}) & T_5(x_k)(Y_k - x_{2,k}) \end{bmatrix}$$

Finally, the 9x9 covariance matrix associated with the measurement is defined as follows:

$$R = diag(3.49E - 6, 5.67E - 5, 5.75E - 6, 5.75E - 6, 7.09E - 7, 7.09E - 7, 7.09E - 7, 7.09E - 7, 7.09E - 7)$$

The above localization algorithm was implemented in MATLAB, where the simulation is based on a predefined setup that is identical in experimentation. A mid and long range IR sensor is used to measure distance of the heat source in the x-axis, while two short range sensors are used to measure distance of the heat source in the y-axis. The thermocouples are mounted in the center and four corners of the plate at an offset of 1 cm from each edge. Figure 2 reveals the experimentation set up of the sensors, which is indistinguishable in simulation.

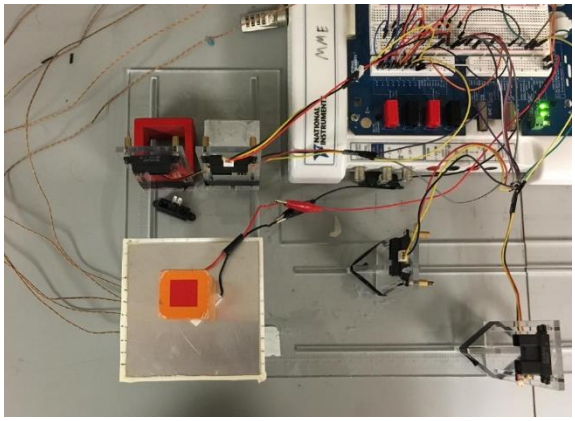

Fig. 2. Sensor fusion set up

Two different placements of the heat source were measured for each localization simulation. The position of the heat source will be placed in the top left quadrant (north-west) and bottom right quadrant (south-east). Depending on the position of the heat source, certain IR sensors weren't utilized in the simulation as the aluminum plate was not within its field of view. For example, if the heat source was placed in the top left quadrant, then the long sensor and short sensor to the right weren't

utilized. In each figure, the actual, predicted, initial estimate and final estimate of the heat source position will be plotted.

A. *Localization using IR Sensors*

For the IR sensors, the short range sensors are 6 cm away from the edge of the plate, while the mid and long range sensors are 12 and 22 cm, respectively, away from the edge of the plate.

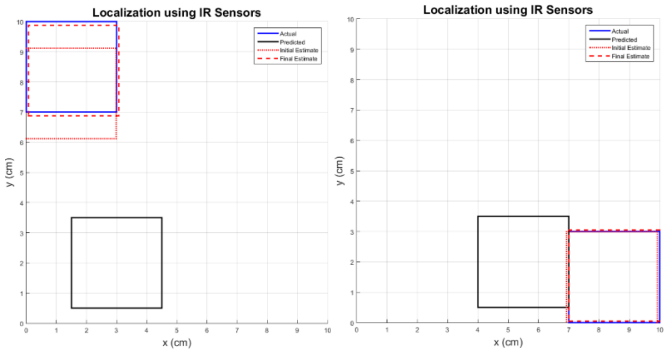

Fig. 3. Localization using IR sensors in simulation

From the above figures, it can be noticed that the estimate attempts to converge to the actual position right from the start. This is more evident in the last case where the predicted location was closer to the actual position as opposed to the first case. Nonetheless, in all cases, the EKF converges to the actual position in very few steps and accurately localizes the position of the heat source at the final time step. The IR sensors are best suited during the transient phase of the heat source given that the sensors are not dependent on temperature. However, the IR sensors will not be utilized if an object is not placed in its field of view. As a result, with the given setup, certain IR sensors will be unable to detect the heat source if placed onto the corners of the aluminum plate. The updated covariance matrix reveals relatively low values which indicate there is high confidence in localizing the position of the heat source using just IR sensors. The updated covariance matrix for each case is shown below:

TABLE I. IR SENSOR COVARIANCE MATRIX

	Heat Source Position	
	North-West	***South-East***
Covariance	$P_k = \begin{bmatrix} 0.0104 & 0 \\ 0 & 0.0101 \end{bmatrix}$	$P_k = \begin{bmatrix} 0.0105 & 0 \\ 0 & 0.0101 \end{bmatrix}$

B. *Localization using Thermocouple Sensors*

The same two cases were evaluated to localize the position of the heat source using only thermocouples. These figures are shown below:

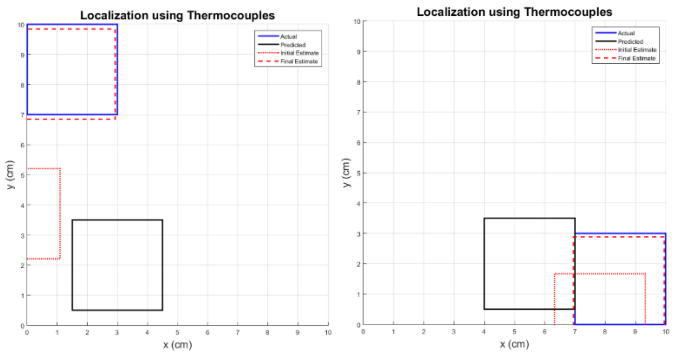

Fig. 4. Localization using thermocouple sensors in simulation

The results indicate that the thermocouples converge at a slower rate than the IR sensors. This can be explained by the lack of reliability of just using thermocouples during the transient phase of the heat source. Thermocouples are heavily dependent on temperature and as such are better suited for steady state scenarios where fluctuations in temperature are minimal. The EKF eventually localizes the position of the heat source at the final time step. The updated covariance matrix can be seen below, where it is evident that the covariance values are much higher than the IR sensors, indicating less confidence in the measurement model of the thermocouples.

TABLE II. THERMOCOUPLE SENSOR COVARIANCE MATRIX

	Heat Source Position	
	North-West	***South-East***
Covariance	$P_k = \begin{bmatrix} 0.0523 & 0.0259 \\ 0.0259 & 0.0329 \end{bmatrix}$	$P_k = \begin{bmatrix} 0.0379 & 0.0317 \\ 0.0317 & 0.0584 \end{bmatrix}$

C. *Localization using Sensor Fusion*

Again, the same two cases were evaluated using both IR sensors and thermocouples. The derived plots are shown below:

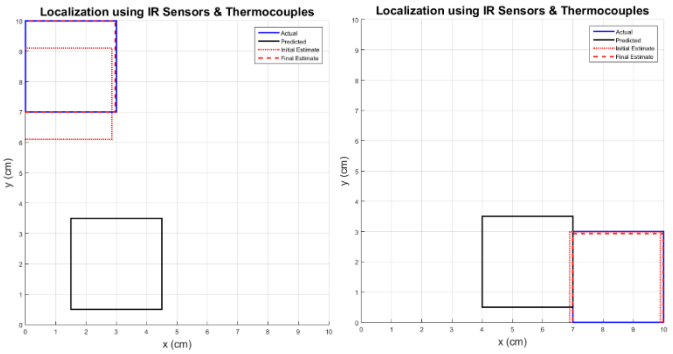

Fig. 5. Localization using sensor fusion in simulation

Combining both sensors results in a convergence time that is in between the two models, however, is more heavily weighted towards the accuracy of the IR sensors. The fused system is able to localize the heat source fairly accurately right from the initial time step, and only performs slightly worse than just using the IR sensors alone. The fused system overcomes the shortcomings from both models as the IR sensors perform well during transient, while thermocouples perform well during steady state.

Aside from the convergence time, another downside of the fused system is the computationally heavy nature of having to rely on both sensor models. The updated covariance matrix can be seen below, where the values are identical to that of the IR sensors.

TABLE III. SENSOR FUSION COVARIANCE MATRIX

	Heat Source Position	
	North-West	***South-East***
Covariance	$P_k = \begin{bmatrix} 0.0104 & 0 \\ 0 & 0.0101 \end{bmatrix}$	$P_k = \begin{bmatrix} 0.0105 & 0 \\ 0 & 0.0101 \end{bmatrix}$

IV. EXPERIMENTATION

The experimental apparatus is composed of an NI ELVIS II+ board, a 10cm by 10cm aluminum plate, and a 1.5 cm by 1.5 cm Peltier module heat source. The aluminum sheet is elevated by PCV casing to eliminate the transfer of heat through convection from the plate to the table, and the Peltier module is stuck to the aluminum plate with the heat side in contact using sticky tack. The sensor system is composed of the five thermocouples and four IR sensors (two short, one medium, and one long) used in the simulation, which are connected to the nine analog input pins on the ELVIS board to record voltage output. The Peltier module is powered by the 5V DC power source on the ELVIS board.

The exact same setup that was carried out during simulation was followed during the experimentation. A tall wooden block was placed on top of the heat source in order to capture the field of view of the IR sensors. Furthermore, the same two heat source positions will be evaluated for each localization method.

A. *Localization using IR Sensors*

Localization of the heat source using just IR sensors are evaluated at the north-west and south-east positions. These figures are shown below.

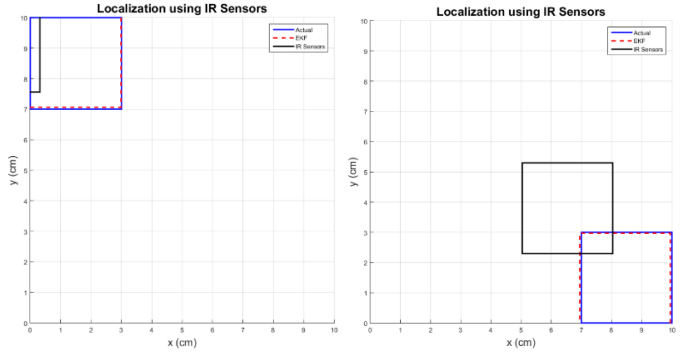

Fig. 6. Localization using IR sensors in experimentation

There exists significant inaccuracy between the simulation and experimental results, especially in the x-direction. Several factors may have influenced the inaccuracy of this model. It was shown in an earlier lab that the use of a wooden block is less accurate than using a metal surface. Additionally, slight deviations in angle from the perpendicular plane between the IR sensor and surface of the block can result in vast changes. Finally, environmental conditions such as lighting in the room may influence and skew the recorded data as well.

B. *Localization using Thermocouple Sensors*

In order to determine the exact location of the heat source using thermocouples, a trilateration technique [5] shown in Figure 7 is used after obtaining the distance measurements from the inverse sensor model.

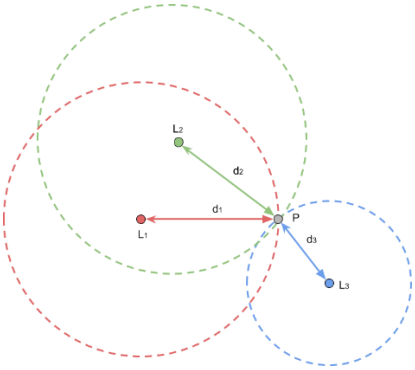

Fig. 7. Trilateration technique [5]

The same cases for position of the heat source as before are evaluated for localizing using just the thermocouples.

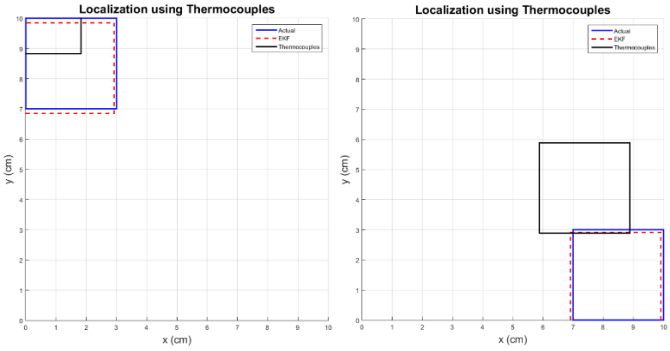

Fig. 8. Localization using thermocouple sensors in experimentation

It can be seen from the generated plots that relying on the thermocouples results in inaccurate data. There exists a large error in localizing the position of the heat source between the simulation and experimental data. The inaccuracy is most likely due to errors that existed during characterization of the thermocouple model in addition to recording the data during the transient phase of the heat source. Additionally, a more robust method would be to consider the difference in voltages between each thermocouple rather than the absolute value. As a result, minor inaccuracies in the experimental setup will exist between the sensor model and raw data captured during the tests.

C. *Localization using Sensor Fusion*

Finally, combining both types of sensors was evaluated to localize the position of the heat source. It is expected that the fusion of both sensors would yield the most optimal results in estimating the position of the heat source. Identical test cases as the previous ones were carried out and the figures can be seen below.

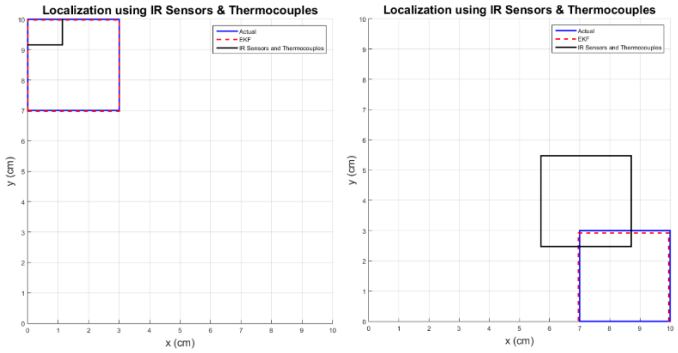

Fig. 9. Localization using sensor fusion in experimentation

It can be observed that the prediction of fusing both sensors yielding the best results is not necessarily valid. This indicates the sensor fusion is only as accurate as the accuracy of individual sensors used. While the simulation results were very accurate in obtaining the true position of the heat source, the experimental results deem otherwise. Since the localization takes into consideration all nine sensors, the errors that exist will be those that are attributed to the IR sensors and thermocouples, respectively. Again, the cost of fusing both sensors involves the inaccuracies associated with each sensor and the non-ideal computation required to locate the heat source.

V. Conclusion

In this lab, a complete sensor fusion system was utilized to locate a heat source produced by a Peltier module on a 10 cm by 10 cm aluminum plate. Specifically, multiple infrared sensors and thermocouples were placed around the physical system to acquire data all the measurements during steady state. The sensors were fused using Kalman Filter techniques to identify the location of the heat source. Heat source localization was examined with solely the IR sensors, solely the thermocouples, and a combination of both sensor types. It was found that the system was able to utilize the sensor models to accurately predict the location of the heat source on the plate.

While the simulations were able to locate the position of the heat source in all three configurations (IR only, thermocouple only, and both), the experimental versions of the same tests had a low degree of accuracy. This is caused by multiple sources of error, including but not limited to the inability to reach steady state, incorrect positions of the sensors themselves, and incorrect thermocouple characterization due to the low change in voltage across the physical domain. Therefore, while the fusion of multiple sensors can result in a much more accurate representation of a system, it is only possible if the experimental setup itself is controlled in such a way that the experimental setup and procedure can still be modeled by the pre-defined sensor models. If this lab was to be repeated, there should be a larger focus on controlling the steady-state conditions of the apparatus.

References

[1] E. Li, “MTE 546 Multi-Sensor Data Fusion Lab Manual”., Learn, University of Waterloo, Jan. 2018. [Online]. [Accessed: Mar. 2020].

[2] “Analog Output Type Distance Measuring Sensor - GP2Y0A41SK0F”., Sharp Corporation, Mar. 2017. [Online]. Available: https://www.pololu.com/product/2464. [Accessed: Mar. 2020].

[3] “Analog Output Type Distance Measuring Sensor - GP2Y0A21YK”., Sharp Corporation, Mar. 2017. [Online]. Available: https://www.pololu.com/product/136. [Accessed: Mar. 2020].

[4] “Analog Output Type Distance Measuring Sensor - GP2Y0A02YK0F”., Sharp Corporation, Mar. 2017. [Online]. Available: https://www.pololu.com/product/1137. [Accessed: Mar. 2020].

[5] A. Zucconi, “Positioning and Trilateration,” Alan Zucconi, Nov. 2018. [Online]. Available: https://www.alanzucconi.com/2017/03/13/positioning-and-trilateration/. [Accessed: Mar. 2020].